

## RESEARCH PAPER

## Oblique Gate Direction During Centrifugal Casting in Artificial Lumbar Disc Model of CP-Ti

Lilik Dwi Setyana<sup>1</sup>, Muslim Mahardika<sup>1,2</sup>, Suyitno<sup>1,2\*</sup><sup>1</sup>Department of Mechanical and Industrial Engineering, Faculty of Engineering, Universitas Gadjah Mada, Yogyakarta, 55281, Indonesia<sup>2</sup>Center for Innovations of Medical Devices, Universitas Gadjah Mada, Yogyakarta, 55281, Indonesia

\*Corresponding author: suyitno@ugm.ac.id, tel.: +6281325017275, Faculty of Engineering / Universitas Gadjah Mada, 55281, Yogyakarta, Indonesia

Received: 16.04.2020

Accepted: 22.06.2020

## ABSTRACT

Oblique gate direction in different angles was hardly applied in centrifugal casting. The purpose of this research was to determine the effects of oblique gate direction in centrifugal casting on density, porosity, roughness, and microstructures in the artificial lumbar disc model. The angles of the oblique gate were ranged from 30° to 150° toward to the runner. The sharp turn of the gate would cause retardations and losses friction that decreased the pressure in molten metal. This process caused the porosity and the surface roughness decreased while the density increased. The product in which the oblique gate direction was the same with the mold rotation was better than the one in the opposite direction. The tangential forces would increase the forces acting on molten metal when entered the mold with the oblique gate direction that same with the mold rotation. Gate with the  $\theta$  of 90° was the most widely used, but the product was better to use the gate with the  $\theta$  of 60° than the product with the  $\theta$  of 90°. Hence, to obtain an artificial lumbar disc model with less porosity, high density, and smooth surface, the oblique gate of 60° should be applied.

**Keywords:** Gating design; Porosity; Centrifugal casting; Artificial lumbar disc model

## INTRODUCTION

The principle of centrifugal casting is the application of forces generated from the centripetal acceleration of a rotating mold to distribute the molten metal into the mold [1]. Centrifugal casting produces a product with limited gas porosity, smooth surface, and accurate dimensions [1, 2]. These characteristics are caused by the distribution of molten metal into the mold cavity, which uses forces resulted from the centripetal acceleration of a mold rotation. The centrifugal force is a function of rotational speed, metal density, and radius [1]. The pressure distribution that controlled by rotational speed affects the shrinkage cavity. The porosity can be reduced by adjusting the rotational speed of more than 180 rpm [3]. Furthermore, increasing the rotational speed affects the increase in pressure, which causes a decrease in defects [4].

Defects on casting products usually happen due to improper in the gating system design (around 90%), and the rest is caused by the manufacturing problems [5, 6]. The product defects such as porosity cannot be avoided but can be controlled. Shrinkage or trapped gas during the cooling process can raise the occurrence of porosity [7-9].

The cross-section, position, and direction of the gate during centrifugal casting are designed to generate products with minimal porosity. Gate shapes that often used are rectangular [10-14] and circular [14-15] cross-section with perpendicular [10-14] and oblique [14] toward the mold cavity. The circular cross-section of the gate has a higher molten metal filling speed rather than the rectangular one [10]. Viscosity increases rapidly in rectangular cross-section, which has a closer gating wall distance to the center of cross-section rather than the circular one. This condition affects porosity, which tends to be more numerous [10]. Research on gate direction in centrifugal casting is still needed so that molten metal enters the mold cavity with high pressure and low turbulence. The high pressure and low turbulence can be obtained by changing geometry, shape, and number of the gates [12, 16].

However, the products of centrifugal casting always have porosity even though rectangular or circular cross-sections of gate shape are used. Gate direction, which same or opposite to the mold rotation, which purpose is to increase the molten metal filling to the mold, still needs further investigations [14]. The rectangular cross-section gate shape with the oblique direction the same as the rotation of the mold was suitable to be implemented in the centrifugal casting product [14]. However, the optimum angle of the oblique gate to be applied in the product is not yet known. The study is conducted to determine the influence of various oblique gate directions toward porosity, density, microstructure, hardness, and surface roughness of the artificial lumbar disc (ALD) model.

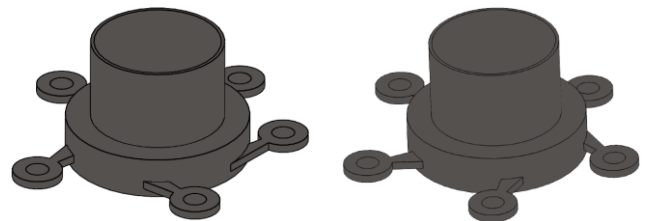
## MATERIAL AND METHODS

Commercial pure titanium (CP-Ti) with composition of 99.72 wt.% Ti, 0.17 wt.% Fe, and 0.11 wt.% gaseous element was used in this research. The composition analysis used EDS (Quanta x50 SEM Series).

The product made in this study was an artificial lumbar disc model (ALD model). It was produced with centrifugal casting as arranged in Fig. 1. The product was set in a variety of oblique gate directions, which shown in  $\theta$  ranged from 30° up to 150°. The  $\theta$  was an angle formed by the axis of the gate and runner. Fig. 1.a showed the positions of the gate with the  $\theta$  of 30°, 45°, 60°, 75°, and 90°. Then the  $\theta$  of 90°, 105°, 120°, 135°, and 150° were shown in Fig. 1.b. The gate direction of 30° up to 75° was the same as the mold rotation. The gate direction of 90° was perpendicular toward the runner. Then the gate direction of 105° up to 150° was opposite with the mold rotation.

The ALD model geometry was shown in Fig. 2.a. The outer diameter was 30 mm, while the radius of the ball-on-socket was 13 mm with 2 mm depth. The gate shape (Fig.2.b) was rectangular cross-section. The cross-sectional geometry area declined gradually, along with the process of molten metal entering the mold. Then, the cross-sectional area of the gate declined gradually from 70 mm<sup>2</sup> to 30 mm<sup>2</sup> with the length of the gate for about 15 mm.

CP-Ti was melted at 1700° C, then poured in an ALD model shell mold. The zirconium-based ceramic material (consisted of 8 layers) was used to create the shell mold. The pouring rate of molten metal was about 0.12 kg s<sup>-1</sup>. Moreover, when molten metal was poured, the mold was rotated in a counterclockwise direction at 60 rpm. The processes were conducted in the vacuum furnace (Flash caster, Japan).



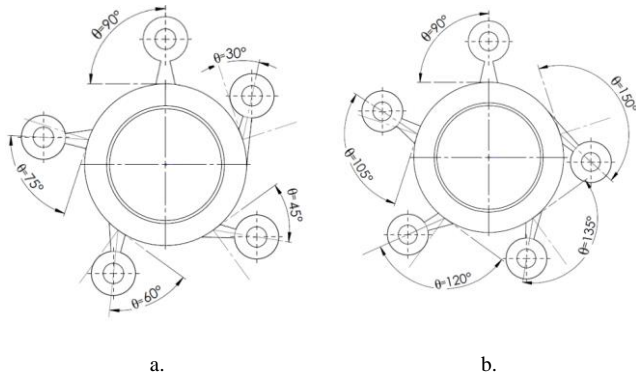


Fig. 1 The schematic arrangement of the oblique gate direction

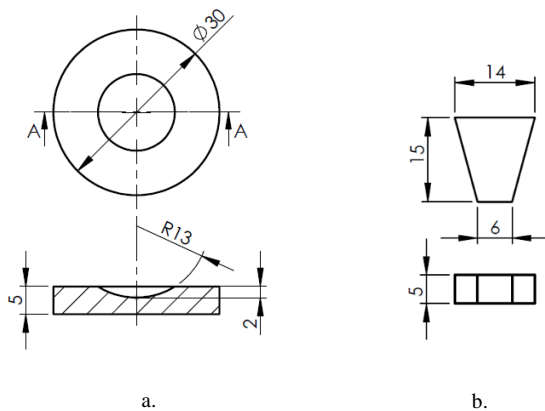


Fig. 2 The geometry of ALD model (a) and gate shape (b)

The observations in this study consisted of shrinkage porosity and microstructures. The shrinkage porosity was observed using a stereo-zoom microscope (SZ-PT, Olympus, Japan) after the in-depth preparation by dye penetrant. Porosity calculations were manually counted using millimeter blocks. Besides, the percentage of porosity was calculated by comparing the porosity area with a total area of the product. The microstructure was observed using a metallurgical microscope (PME3, Olympus, Japan). Specimen preparation was done with sandpapers (grade #100 to #8000) to produce a smooth surface, then polished by the autosol. Kroll solution was used to bring out the microstructure (etching process).

The measurements consisted of hardness, surface roughness, and density. The hardness was measured from the sub-surface to the inner of a cross-sectional spanning product using a microhardness tester (HMV-M3, Shimadzu, Japan). The distance of each point test of hardness was arranged for 50  $\mu\text{m}$ . Then, the load was set for 2 N. Profilometer (Surfcorder SE 1700, Fowler) was used for testing the surface roughness (Ra). The density was calculated by dividing the weight with the volume of the product. The equipment used to measure the weight in this research was analytical balancing (Sartorius AG Gottingen LC-12018).

## RESULTS AND DISCUSSION

### Results

The ALD model, which produced using centrifugal casting with the variation of oblique gate direction is shown in Fig. 3. All oblique gate directions, ( $\theta$  range from 30° up to 150°) produce a complete filling casting. Fig. 4 shows defects on the product surface. The surface shrinkage porosities (A) and pinholes (B) can be seen on the surface. The surface shrinkage porosities are seen with an irregular shape

that has a length and wide about 3 mm and 1 mm, respectively. The pinhole tends to congregate with a diameter of about 0.1 mm. It is also reported in prior research [17]. The product with  $\theta$  of 60° has the least amount of surface shrinkage and pinholes. On the other hand, the product with  $\theta$  of 150° has the largest surface shrinkage and pinholes, among others.



Fig. 3 The ALD model product

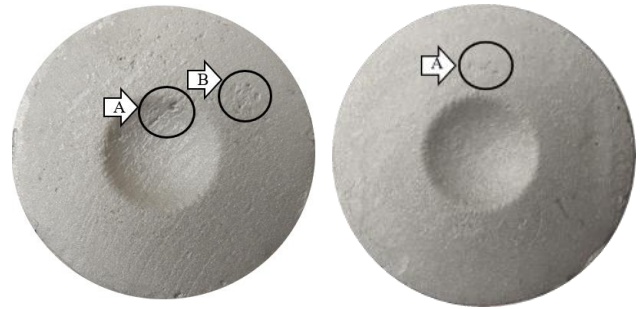
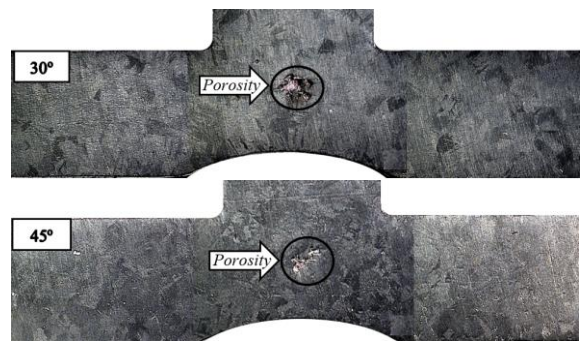


Fig. 4 The pinhole and surface shrinkage defects

Fig. 5 and Fig. 6 shows the internal porosity of ALD model products with  $\theta$  of 30° up to 150°. The porosities are found in the mid area between the thickness of the products. The porosity with  $\theta$  of 30° up to 90° tends to congregate with a size of about 100-200  $\mu\text{m}$ . Meanwhile, the porosity with  $\theta$  of 105° up to 150° tends to spread in size about 50-100  $\mu\text{m}$ .

Fig. 7 shows the enlargement of the internal shrinkage porosity of the product with  $\theta$  of 150°. It has an irregular shape in various sizes (50-200  $\mu\text{m}$ ). Some of the internal shrinkage porosity has a crack tail. Several adjacent porosities are connected by the crack tail.

Fig. 8 describes the number of porosity areas. The percentage porosity area with  $\theta$  of 30° up to 150° are 0.65, 0.47, 0.34, 0.36, 0.49, 0.50, 0.59, 0.82, and 0.92% respectively. The porosity area tends to decrease along with the increase of the  $\theta$  (30° up to 60°). On the contrary, for the  $\theta$  that is more than 60°, the porosity area tends to increase. The  $\theta$  of 150° has the highest percentage of porosity area (0.92%), while the  $\theta$  of 60° has the lowest percentage of porosity area (0.34%).



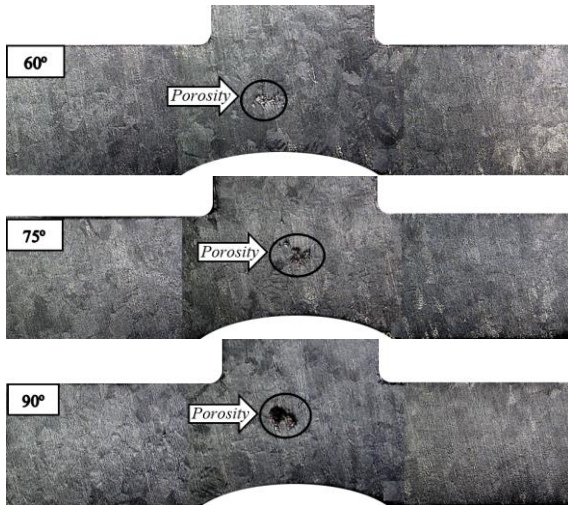


Fig. 5 The shrinkage porosity on product with various oblique gate directions (the  $\theta$  of 75° up to 90°)

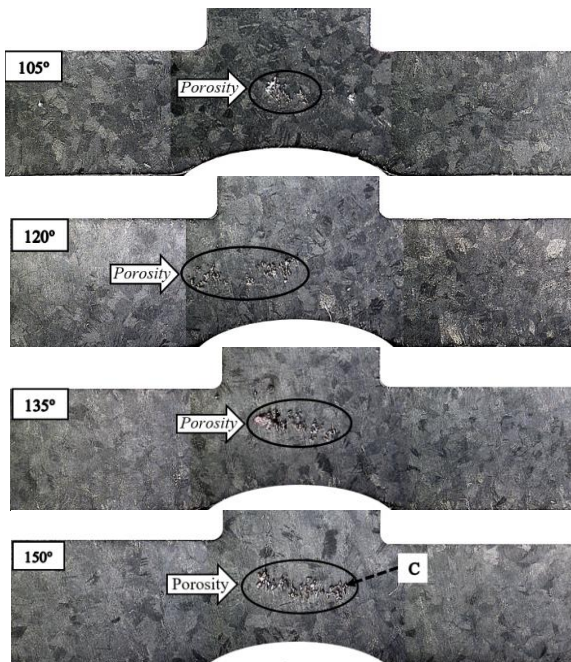


Fig. 6 The shrinkage porosity on product with various oblique gate directions (the  $\theta$  of 105° up to 150°)

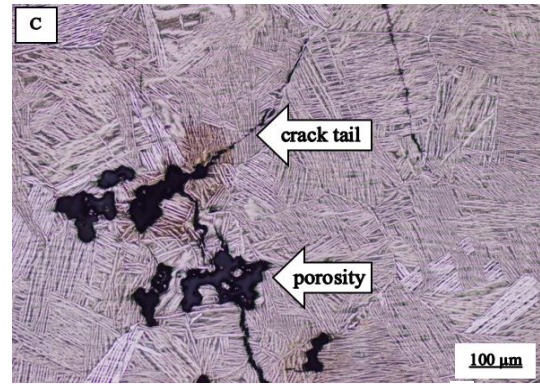


Fig. 7 An enlargement of shrinkage porosity (C in products  $\theta$  of 150°)

The microstructure consists of  $\alpha$  morphologies and equiaxed prior  $\beta$  grains in all kinds of oblique gate direction (Fig. 9). It is supported by the previous result [18]. The types of  $\alpha$ -morphologies are known as  $\alpha$ -case (a), prior  $\beta$  grain boundaries (b), and widmanstatten  $\alpha$  (c). The morphologies of grain have the same characteristics as the previous research [19].

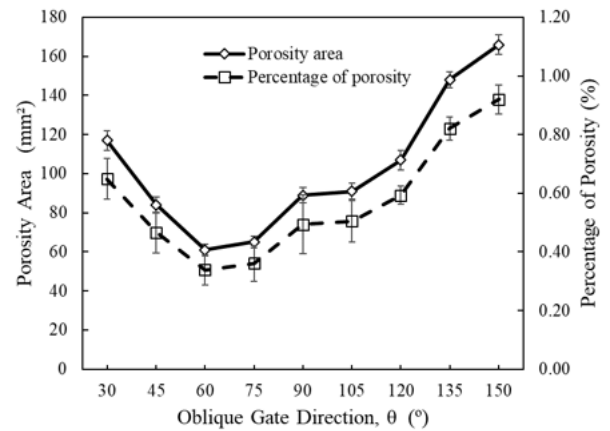


Fig. 8 The porosity area of ALD model

The  $\alpha$ -case (Fig. 9.a) is formed in the sub-surface with a thickness of about 100  $\mu\text{m}$ . The thickness of  $\alpha$ -case in the product with the variate gate direction has a range from 50  $\mu\text{m}$  to 250  $\mu\text{m}$ . The thickness of  $\alpha$ -case on the product with  $\theta$  of 30°, 45°, 60°, 75°, and 90° are 200, 150, 50, 100, and 150  $\mu\text{m}$  respectively. Then the  $\alpha$ -case on the product with  $\theta$  of 105°, 120°, 135°, and 150° are 150, 200, 250, and 250  $\mu\text{m}$  respectively. The  $\alpha$ -case on the product with a gate direction of 120° up to 150° has a crack for about 150-500  $\mu\text{m}$  in length. Meanwhile, the  $\alpha$ -cases on the product with other oblique angles have no crack.

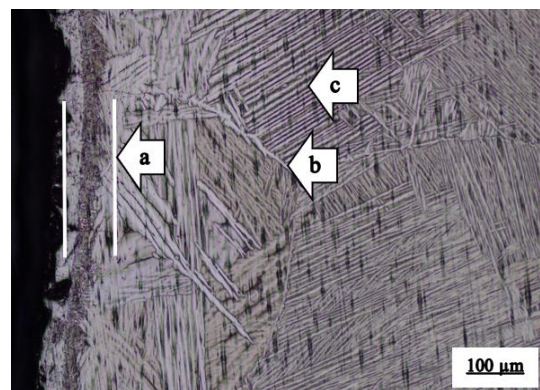


Fig. 9 The microstructures in the sub surface of product with the  $\theta$  of 75°

The ALD density with various gate directions is shown in Fig. 10. The density for the  $\theta$  of  $30^\circ$  up to  $60^\circ$  tends to increase from  $4.514$  to  $4.519 \text{ g cm}^{-3}$ . Whereas, for the  $\theta$  of  $60^\circ$  up to  $150^\circ$ , the density decreases from  $4.519$  to  $4.510 \text{ g cm}^{-3}$ . The density increases up to  $0.11\%$  on a product with the  $\theta$  of  $60^\circ$  compared with the density on the  $\theta$  of  $30^\circ$ . On the contrary, the density decreases to  $0.20\%$  on the product with the  $\theta$  of  $150^\circ$  compared with the density on the  $\theta$  of  $60^\circ$ .

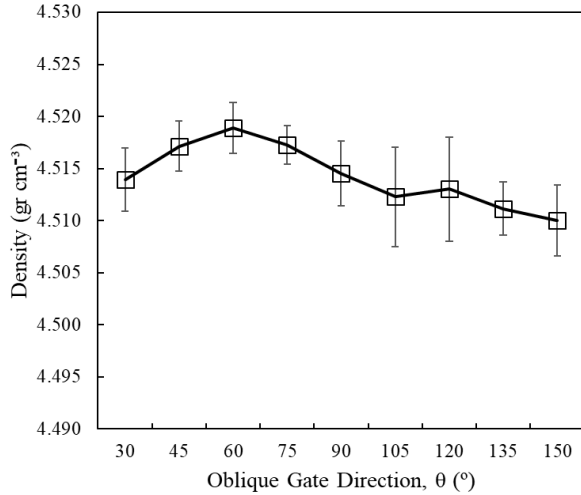


Fig. 10 The density of ALD model

The hardness of the ALD model is seen in Fig. 11. The hardness in the sub-surface with the  $\theta$  of  $30^\circ$  is  $766 \text{ VHN}$ . Then on the distance of  $0.2 \text{ mm}$ , it drops to  $332 \text{ VHN}$ . Continuously on the distance of  $0.05 \text{ mm}$ , the hardness is  $223 \text{ VHN}$ . Meanwhile, after the distance of  $0.05 \text{ mm}$  the hardness tends to stabilize in  $210 \text{ VHN}$ . In general, the hardness with  $\theta$  of  $30^\circ$  up to  $150^\circ$  from the sub-surface to the inner has the same trend. However, some differences occur in the sub-surface ( $\alpha$ -case), as seen in Fig. 12. The hardness with the  $\theta$  of  $30^\circ$  to  $60^\circ$  is decreasing from  $766 \text{ VHN}$  to  $644 \text{ VHN}$ . Meanwhile, the hardness on the product with  $\theta$  of  $75^\circ$  to  $150^\circ$  is  $701 \text{ VHN}$  to  $766 \text{ VHN}$ .

The average hardness in the sub-surface with oblique gate direction opposite to the mold rotation ( $105^\circ$ - $150^\circ$ ) is higher than the average hardness with the same direction to the mold rotation ( $30^\circ$ - $75^\circ$ ). The enhancement of the average hardness is up to  $7\%$ .

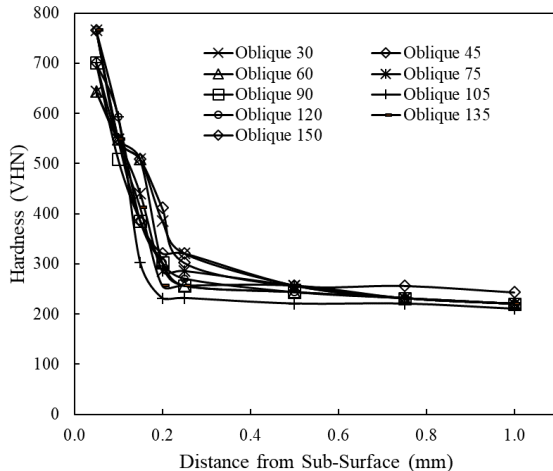


Fig. 11 The hardness of ALD model

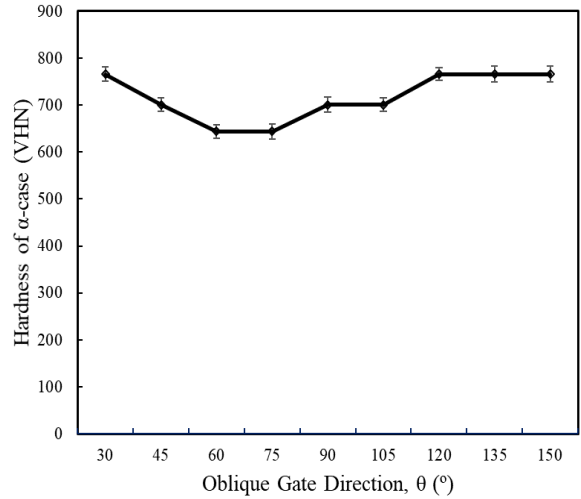


Fig. 12 The hardness of  $\alpha$ -case

The surface roughness ( $R_a$ ) of the product is ranged from  $3.9$  to  $5.5 \mu\text{m}$ . (Fig.13). The surface roughness for the  $\theta$  of  $30^\circ$  to  $60^\circ$  tends to decrease from  $5.5$  to  $3.9 \mu\text{m}$ . Then it increases from  $3.9$  to  $5.5 \mu\text{m}$  on the  $\theta$  of  $60^\circ$  to  $150^\circ$ . The  $R_a$  with  $\theta$  of  $60^\circ$  decreases  $30\%$  compared with  $R_a$  on the  $\theta$  of  $30^\circ$ .

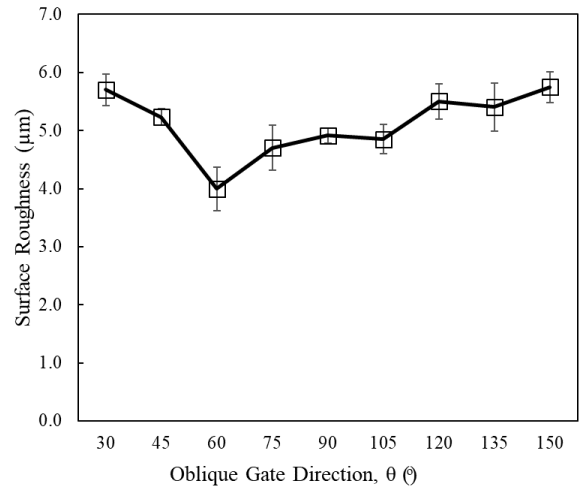


Fig. 13 The surface roughness of ALD model

Discussion

Gates with  $\theta$  of  $30^\circ$  to  $75^\circ$  are the gates with the same direction to the mold rotation. Gate with  $\theta$  of  $90^\circ$  is perpendicular toward the runner. Moreover, gates with  $\theta$  of  $105^\circ$  to  $150^\circ$  are the gates with the opposite direction to the mold rotation.

Porosity area and surface roughness tend to decrease along with the  $\theta$  from  $30^\circ$  up to  $60^\circ$ , then increase for the  $\theta$  is more than  $60^\circ$  ( $60^\circ$  up to  $150^\circ$ ). Meanwhile, the density for the  $\theta$  of  $30^\circ$  to  $60^\circ$  tends to increase, then decreases for the  $\theta$  of  $60^\circ$  to  $150^\circ$ .

The forces acting on molten metal when entering a mold cavity with oblique gate are centrifugal and tangential. The magnitude of centrifugal force is the same for all oblique gates in which direction is away from the center. Meanwhile, the tangential force is different depending on the oblique gate directions. The tangential force at the oblique gate directions which same to the mold rotation ( $\theta$ :  $30^\circ$  to  $75^\circ$ ), is positive. The magnitude of oblique gate directions is directly proportional to the tangential force. It will increase the pressure and velocity of the molten metal when entering the mold. While the tangential force at the oblique gate directions which opposite to the mold rotation ( $\theta$ :  $105^\circ$  to  $150^\circ$ ), is

negative. It will reduce the velocity and pressure of the molten metal when entering the mold.

Product with  $\theta$  of  $30^\circ$  up to  $60^\circ$  shows the increasing mechanical properties. Product with  $\theta$  of  $60^\circ$  has the lowest percentage of porosity area (0.34%), the smoothest surface (3.9  $\mu\text{m}$ ), and the highest density (4.519  $\text{g cm}^{-3}$ ). It is caused by the total of centrifugal and tangential force acting on molten metal when entering the mold is bigger than forces on other gate directions. The pressure and velocity of molten metal become the highest when entering the mold. Besides, the gate direction allows molten metal to enter the mold cavity easily. It is caused by small retardation and losses friction. The increasing pressure and velocity of molten metal reduce the internal shrinkage porosity that automatically increases the density. The porosity tends to congregate with a size of about 50-100  $\mu\text{m}$  without a crack tail. The shape and distribution of pores have a significant influence on the mechanical characteristics of materials [20]. The pressure of the molten metal to the wall cavity increases due to the high pressure when pouring. It causes a smooth surface.

Gate with  $\theta$  of  $90^\circ$  is perpendicular toward the runner. This direction is the most widely used in casting [10-14]. The pressure and velocity of molten metal when entering the mold in this direction is determined by centrifugal force. The porosity formed in this direction is lesser than porosity in the opposite gate directions toward the mold (the  $\theta$  of  $105^\circ$  up to  $150^\circ$ ). In the pouring process, the molten metal has less retardation and friction to enter the mold cavity because there are no sharp turns. There is no crack in the  $\alpha$ -case with a thickness of about 150  $\mu\text{m}$ .

Product with  $\theta$   $90^\circ$  up to  $150^\circ$  shows the decreasing mechanical properties. Product with the  $\theta$  of  $150^\circ$  has the highest percentage of porosity area (0.92%), roughest surface (5.5  $\mu\text{m}$ ), and lowest density (4.510  $\text{g cm}^{-3}$ ). Gate with the  $\theta$  of  $150^\circ$  is opposite to the mold rotation. The tangential force in the gate direction is negative. Therefore, it decreases the total forces acting on molten metal. The pressure and velocity on molten metal at  $\theta$  of  $150^\circ$  is the lowest. The pressure is the basic indicator that determines the shrinkage cavities distribution [3]. When the molten metal's pressure is low, it induces shrinkage porosities that directly decrease the density. Also, this gate direction has a sharp turn that causes the molten metal to encounter many retardations in entering the mold cavity. The retardations generate losses of friction between molten metal and gate wall. The greatest retardation occurs in the gate direction of  $150^\circ$ . Losses friction causes the molten metal's pressure to decrease, so it needs longer filling time to enter the mold cavity. The sharp turn also causes a turbulent flow. The turbulent flow will trap the air, then bring it back to molten metal [21]. It consequently induces porosities [22]. The porosity with the  $\theta$  of  $150^\circ$  tends to spread in the irregular form with a crack tail. The low pressure also causes the pressure of molten metal to the wall cavity is less, which resulted in the roughness on the surface (5.5  $\mu\text{m}$ ). Besides, the low pressure causes the sub-surface of the product to have the thickest  $\alpha$ -case, among other directions. The thick  $\alpha$ -case will easily bring out a crack. The  $\alpha$ -case is hard and brittle with a high-stress concentration [23], so cracking happens easily.

The microstructure formed in any of gate directions tends to be similar, which consists of equiaxed prior  $\beta$  grains and  $\alpha$  types. The differences in the cooling rate caused by the differences in gate angles do not affect the type of microstructure. The pressure, velocity or friction also do not affect the microstructure, nor affects the thickness of the  $\alpha$  case. The microstructure on the sub-surface is transformed from a bright coarse grain to become fine grains in the inner area. This structure is similar to previous research [14].

The hardness in all products (any oblique gate directions) from the sub-surface until the distance of more than 0.05 mm relatively have the same trend. On the sub-surface region, an  $\alpha$ -case is formed with a thickness of 50 up to 300  $\mu\text{m}$ . Hardness of  $\alpha$ -case is 644 up to 766 VHN, which caused by the oxygen contamination and finer microstructure on the surface [24]. The hardness is particularly influenced by the kind of phase of the microstructure [25]. Oxygen can extend the  $\alpha$  phase region, which shows that  $\alpha$  phase will be easily formed with increasing oxygen content [26]. This is confirmed with the results of a study [14, 23]. The  $\alpha$ -case on the product with the opposite gate direction of the mold rotation is harder and thicker than the same one. This condition happens because the product with same direction has a high pressure and velocity, which has a higher cooling rate compared to the opposite one during the solidification process. A higher cooling rate prevents oxygen diffusion occurs so that the  $\alpha$ -case is thin [26].

## CONCLUSION

The conclusions of this research are:

1. The product in which the gate direction is the same with the mold rotation is better than the one in the opposite direction because the tangential forces will increase the forces acting on molten metal when entering the mold with the gate direction the same with the mold rotation.
2. The sharp turn of the gate will cause retardations and losses friction that will decrease the pressure in molten metal, which causes the porosity and the surface roughness decrease while the density increases.
3. Gate with the  $\theta$  of  $90^\circ$  (perpendicular toward the runner) is the most widely used in centrifugal casting, but the product is better to use an oblique gate with the  $\theta$  of  $60^\circ$  than the product with the  $\theta$  of  $90^\circ$ .
4. The oblique gate of  $60^\circ$  is the best direction to be implemented in the manufacture of artificial lumbar disc model.

**Acknowledgments:** The research was funded under dissertation grant by the Indonesian Ministry of Finance through Lembaga Pengelola Dana Pendidikan (LPDP). We thank the Department of Mechanical and Industrial Engineering Universitas Gadjah Mada for testing and observation equipments.

## REFERENCES

1. W.S. Ebhota, A.S. Karun, F.L. Inambao: International Journal of Materials Research, 107(10), 2016, 1-10. <https://doi.org/10.3139/146.111423>
2. S. Wu, Q. Xu, X. Xue: Advanced Materials Research, 317-319, 2011, 456-459. <https://doi.org/10.4028/www.scientific.net/AMR.317-319.456>
3. Y. Ling, J. Zhou, H. Nan, L. Zhu, Y. Yin: Journal of Materials Processing Technology, 251, 2018, 295-304. <https://doi.org/10.1016/j.jmatprotec.2017.08.025>
4. T. Prayoga, R. Dharmastiti, F. Akbar, Suyitno: Journal of Mechanical Science and Technology, 32 (1), 2018, 149-156. <https://doi.org/10.1007/s12206-017-1216-8>
5. A. Vegda, S. Bhingradiya, K. Faldu, P. Gandhi, M. Shah: International Journal of Scientific & Engineering Research, 9(1), 2018, 1222-1228.
6. S.L. Nimbalkar, R.S. Daluba: Perspectives in Science, 8, 2016, 39-42. <https://doi.org/10.1016/j.pisc.2016.03.001>
7. Sutiyo, Suyitno, M. Mahardika, A. Syamsudin: Archives of Foundry Engineering, 16 (4), 2016, 157-162. <https://doi.org/10.1515/afe-2016-0102>
8. B.H. Hu, K.K. Tong, X.P. Niu, I. Pinwill: Journal of Materials Processing Technology, 105(1-2), 1999, 128-133. [https://doi.org/10.1016/S0924-0136\(00\)00546-X](https://doi.org/10.1016/S0924-0136(00)00546-X)
9. J.K. Kuo, P.H. Huang, H.Y. Lai, J.R. Chen: International Journal Advance Manufacture Technology, 92(1-4), 2017, 1093-1103. <https://doi.org/10.1007/s00170-017-0198-0>
10. P. Suwankan, N. Sornsuwit, N. Poolthong: Key Engineering Materials, 659, 2015, 647-651. <https://doi.org/10.4028/www.scientific.net/KEM.659.647>
11. M. Gadalla, R. Habingreither, R. Cook: The Minerals, Metals and Materials Society, 55, 2007, 39-45.
12. M. Masoumi, H. Hu, J. Hedjazi, M.A. Boutorabi: American Foundry Society, 05-152(2), 2005, 1-12.
13. B.H. Hu, K.K. Tong, X.P. Niu, I. Pinwill: Journal of Materials Processing Technology, 105, 2000, 128-133. [https://doi.org/10.1016/S0924-0136\(00\)00546-X](https://doi.org/10.1016/S0924-0136(00)00546-X)
14. L.D. Setyana, M. Mahardika, Sutiyo: Acta Metallurgica Slovaca, 25(3), 2019, 193-202. <https://doi.org/10.12776/ams.v25i3.1315>
15. R. Ahmad, M.Y. Hasyim: Archives of Metallurgy and Materials, 56(4), 2011, 991-997. <https://doi.org/10.2478/v10172-011-0109-6>
16. O. Akinlabi, A. Ayodele: Acta Metallurgica Slovaca, 21(2), 2015, 135-141. <https://doi.org/10.12776/ams.v21i2.567>
17. J.K. Kuo, P.H. Huang, H.Y. Lai, W.J. Wu: The International Journal of Advanced Manufacturing Technology, 100, 2019, 529-540. <https://doi.org/10.1007/s00170-018-2737-8>
18. K.M. Ibrahim, M. Mhaede, L. Wagner: Transactions of Nonferrous Metals Society of China, 21(8), 2011, 1735-1740. [https://doi.org/10.1016/S1003-6326\(11\)60923-0](https://doi.org/10.1016/S1003-6326(11)60923-0)
19. M.J. Bermingham, S.D. Donald, M.S. Dargusch, D.H. John: Journal Material Research, 23(1), 2008, 97-104. <https://doi.org/10.1557/JMR.2008.0002>
20. J. Bidulská, R. Bidulský, M. A. Grande, T. Kvackaj: Materials, 12(22), 2019, 3724. <https://doi.org/10.3390/ma12223724>

21. B.D. Lee, U.H. Baek, J.W. Han: Journal of Materials Engineering and Performance, 16 (1), 2012. <https://doi.org/10.1007/s11665-011-0111-1>
22. J.R. Brevick: Die Casting Engineering, 5, 1997, 42–46.
23. W.J. Boettinger, M.E. Williams, S.R. Coriell, U.R. Kattner, B.A. Mueller: Metallurgical and Materials Transactions B, 31(B), 2000, 1-9. <https://doi.org/10.1007/s11663-000-0026>
24. X. Feng et.al: Journal of Materials Science & Technology, 32, 2016, 362-371. <https://doi.org/10.1016/j.jmst.2015.12.010>
25. S. Darmo, L. D. Setyana, Tarmono, N. Santoso: IOP Conf. Series: Materials Science and Engineering, 384, 2018, 1-4. <https://doi.org/10.1088/1757-899X/384/1/012017>
26. Y. Ma et.al: Journal of Materials Science & Technology, 26(2), 2010, 131-135. [https://doi.org/10.1016/S1005-0302\(10\)60021-7](https://doi.org/10.1016/S1005-0302(10)60021-7)